

# SL-CycleGAN: Blind Motion Deblurring in Cycles using Sparse Learning

Ali Syed Saqlain  
NCEPU, Beijing, China  
ncepu.edu.cn

1164300014@ncepu.edu.cn

Li-Yun Wang  
Portland State University, U.S.A  
pdx.edu

liyuwang@pdx.edu

Fang Fang  
NCEPU, Beijing, China  
ncepu.edu.cn

ffang@ncepu.edu.cn

## Abstract

In this paper, we introduce an end-to-end generative adversarial network (GAN) based on sparse learning for single image blind motion deblurring, which we called SL-CycleGAN. For the first time in blind motion deblurring, we propose a sparse ResNet-block as a combination of sparse convolution layers and a trainable spatial pooler  $k$ -winner based on HTM (Hierarchical Temporal Memory) to replace non-linearity such as ReLU in the ResNet-block of SL-CycleGAN generators. Furthermore, unlike many state-of-the-art GAN-based motion deblurring methods that treat motion deblurring as a linear end-to-end process, we take our inspiration from the domain-to-domain translation ability of CycleGAN, and we show that image deblurring can be cycle-consistent while achieving the best qualitative results. Finally, we perform extensive experiments on popular image benchmarks both qualitatively and quantitatively and achieve the record-breaking PSNR of 38.087 dB on GoPro dataset, which is 5.377 dB better than the most recent deblurring method.

## 1. Introduction

Motion blur is one of the most recursive problems of paramount importance in the field of computer vision and digital photography. It is mainly caused by the streaking of fast moving objects in an image or video frames, also some of the other reasons could be the camera shake or long exposure time [37, 47, 60, 68, 74]. An interesting way to understand motion blur is to understand the concept of relative motion, *e.g.*, motion of an object relative to the observer in an instance of time. During a single exposure time, the image captured by the camera, especially when an object is moving in the captured image may represent a scene over a continuous interval of time. Such motion of an object in a captured image, causes motion blur artifacts or more specifically displacement of pixels. Removal of motion blur from the images, is to obtain the clean sharp images from the blurry inputs by minimizing the mismatch between the

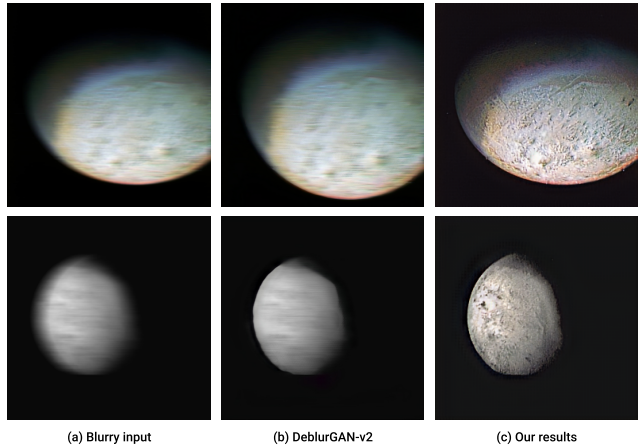


Figure 1. Photos of Triton by Voyager, Neptune’s satellite. Images taken from NASA’s official website [46]. From left to right: first column, the blurry input, second, the restored results from [36] and finally, our restored results. The synthetic motion blur in the input images is of magnitude of 96 pixels with 0 degrees angle.

latent sharp image and the restored sharp image. Considering the fact, that motion blur in real-world is commonly shift-variant or non-uniform in nature, and the depth or the density of blur may fluctuate over different regions of an image [6, 12, 14, 22]. The earlier blind deconvolution methods assume the estimation of unknown blur kernel by studying image priors [33, 40, 51, 69, 73, 82, 84], Weiner deconvolution [33, 71], or Richardson-Lucy bayesian approach [58]. However, such outdated methods inevitably need the hand-crafted image priors, while not to mention the cost of computational resources and the exponential increase in complexity.

Thanks to the recent advancements in deep learning, and its tremendous feature learning ability from training to testing in blind image deblurring task [45, 59, 63, 66, 78], we do not need to rely on conventional approaches anymore. Especially, considering the revolution that GANs [18] have brought not only in general-purpose computer vision tasks [29, 30], but also in blind motion deblur-

ring task [5, 35, 36, 61, 80]. Despite the colossal success of GANs in blind motion deblurring, the quality of restored images from the blurry inputs is still straggling. No doubt, either scale-wise stacking of convolution layers [16, 17, 45, 48, 59, 63, 66, 76, 78] or versions of GAN-based DeblurGAN models [35, 36] have significantly improved the performance of restoration both in terms of qualitative and quantitative analysis.

To address the problem of non-uniform blind image deblurring, and to propose such a GAN-based blind image motion deblurring network, that, unlike other GAN-based models does not treat the restoration of sharp image as a linear end-to-end process from input to output. Instead, our proposed approach (SL-CycleGAN) treats blind motion deblurring as a domain-to-domain translation problem. What’s even more interesting is, we take the inspiration for this research from the sparse representation learning of [1], not only this, but we also combine Hawkins *et al.* [21] research on Hierarchical temporal memory (HTM) and “A thousand brains: A new theory of intelligence” by Jeff Hawkins [20]. By observing other GAN-based state-of-the-art methods for blind motion deblurring [7, 35, 36], the results achieved by our proposed framework outperform state-of-the-art motion deblurring methods, and speak for themselves both qualitatively and quantitatively. Fig. 1 shows the supreme reconstruction ability of our proposed method against DeblurGAN-v2 [36] on low-light space images.

Our contributions in this research paper are summarized as follow:

- **The Framework:** There is no denial that, GAN-based models are notorious in nature when it comes to problems such as mode-collapse and vanishing gradient [3, 56]. Therefore, a thoughtful choice of network that is able to tackle such issues is of vital importance. We adopt CycleGAN [83] for its amazing ability of domain-to-domain translation. Unlike, other GAN-based models for blind motion deblurring, our proposed network is cycle-consistent, that means, not only the generators of our network are able to deblur the blurry input but also they are able to reconstruct synthetic non-uniform motion blur similar to the original blurry input.
- **Sparse Convolutions:** Our second contribution is the adoption of intrinsic advantages of high dimensional sparse representation through sparse convolutions, similar to [1]. The primary reason why we choose sparse convolutions over standard convolutions layers in our proposed generator architecture is, sparse representations are more robust to noise and interference.
- **HTM:** Hierarchical Temporal Memory (HTM) is an algorithm that models how neocortex of a human brain

performs complex world calculations such as understanding of visual patterns, context of spoken language, perceiving the information through touch and other sensory organs [21]. Our final contribution is, utilizing a trainable HTM spatial pooler such as k-winner [1] to replace non-linearity  $\text{ReLU}(\cdot)$  with k-winner in the residual-block of the generator network. The reason of k-winner as a replacement for classic ReLU is, it is naturally more robust to variance in noise and interference from random signals. In addition, k-winner constraints the output of each layer to the most active non-zero units.

## 2. Related work

### 2.1. Motion Deblurring

Earlier methods treat blind motion image deblurring as an image deconvolution problem [11, 15, 60, 72]. Similarly, sparse-based methods before the introduction of CNNs explore the sparse image gradients in the input blurry images [34, 40, 50, 54, 64, 72, 73]. Meanwhile, other similar motion deblurring approaches focus more on the advantages of patch-wise estimation [44] and estimation of dark channel image priors [51]. However, these conventional image deconvolution methods assume the blur to be uniform, while real-world blur is mostly non-uniform or shift-variant. Since the introduction of deep learning and CNNs, the blind motion deblurring community has seen exponential improvement in the quality of restored sharp images such as [17, 48, 63]. Nah *et al.* [45] proposed a deep scale-wise convolution network for dynamic scene motion deblurring. Unlike conventional deconvolution methods, [45] eliminates the need of knowing explicit blur kernel in advance. Similarly, Schuler *et al.* [59] proposed deep CNN network for blind motion deblurring in a coarse-to-fine scheme. Tao *et al.* [66] proposed an encoder-decoder scale-wise recurrent network architecture for blind motion deblurring. Zhang *et al.* [78] proposed a sequential CNN architecture for dynamic scene deblurring, while achieving impressive results in comparison with [45] and [66]. Gao *et al.* [16] proposed a parameter selective sharing scheme, and a multi-scale encoder-decoder model with nested skip connections for dynamic scene deblurring. Cai *et al.* [7] proposed a dynamic scene motion deblurring network that investigates the dark and bright channel image priors in the input blurry images.

### 2.2. GANs for Motion Deblurring

Generative adversarial networks (GANs) [18] since their introduction, have been widely used for computer vision tasks. A GAN architecture is a deep neural network that consists of mainly a generator  $G$  and a discriminator  $D$ . A generator network that generates a fake generated sample

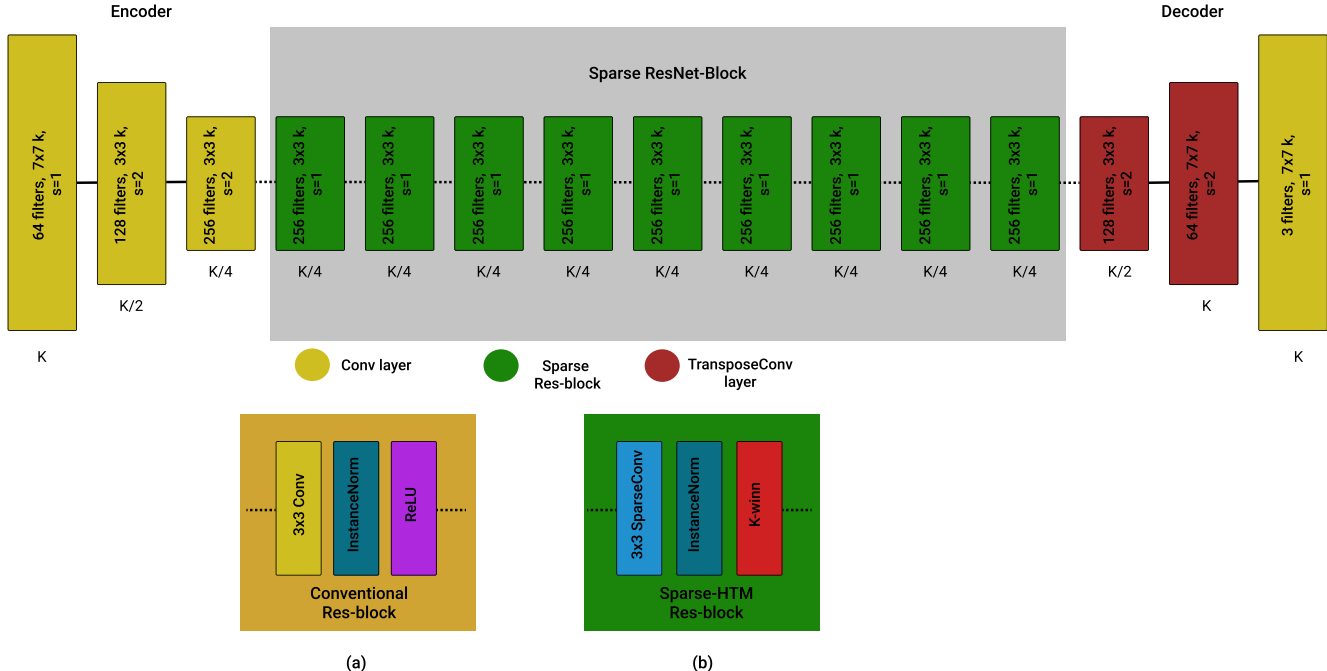


Figure 2. Architecture of SL-CycleGAN generators. The encoder block of the generator contains strided convolutions layers with stride of  $\frac{1}{2}$ . Each convolution layer in the encoder block and TransposeConv layer in the decoder block is followed by the InstanceNorm and non-linearity ReLU. Besides, the generators network contains 9-residual blocks. Fig. 2a shows the conventional Res-block architecture with Conv layers, InstanceNorm, and ReLU, while Fig. 2b shows the modified Res-block with Sparse-Conv layer, InstanceNorm, and ReLU is replaced by HTM k-winn. Each Sparse Res-block contains a Sparse-conv layer, InstanceNorm, and k-winn.

$G(z)$ , normally takes a random noise vector  $z$  as an input, more specifically in a deblurring scenario, an input blurry image is passed through the generator network and it outputs a fake sharp version of the input image. While the discriminator network acts as a classifier by discriminating between the real data sample  $x$  and the generated sample  $G(z)$ . Both of these adversaries play a minimax game and keep getting better and better. Theoretically, the main goal of such adversarial network is to approximate the generated distribution  $p_z$  to the real data distribution  $p_d$ . The minimax objective function for GANs can be formulated as,

$$\min_G \max_D [\mathbb{E}_{x \sim p_d} \log(D(x))] + [\mathbb{E}_{z \sim p_z} \log(1 - D(G(z)))] \quad (1)$$

Based on the success of GANs, Kupyn *et al.* [35] proposed a conditional GAN-framework (DeblurGAN) for single image blind motion deblurring. DeblurGAN consists of a generator and a discriminator network for deblurring task, while utilizing Wasserstein loss function [4] and optimization criteria with an additional gradient penalty to tackle GAN related issues [19]. Kupyn *et al.* [36] proposed the improved version of previous DeblurGAN [35], called DeblurGAN-v2. The DeblurGAN-v2 modified the original architecture of the generator network of DeblurGAN by incorporating the Feature pyramid network (FPN) [43] for

improved quality. Similarly a relativistic local and global discriminator network is introduced [28] with Inception-ResNet-v2 [65] as a backbone of the network. Shao *et al.* [61] proposed a GAN-based deblurring framework that explores the dark and bright channel image priors. Asim *et al.* [5] proposed a blind image deblurring network based on deep generative priors. However, their proposed method lack the experimental analysis on real-world benchmarks for deblurring. Zhang *et al.* [80] proposed a image deblurring and denoising network by combining the noisy and blurry image pairs acquired in a burst. Similarly, Lin *et al.* [42] deployed a GAN-based framework for blind dynamic scene deblurring. Several other approaches either exploit the network architecture in scale-wise convolutions [2, 26, 81], or the deep generative and discriminative priors [41, 57] for dynamic scene blind motion deblurring.

### 3. SL-CycleGAN Network Architecture

The detailed architecture of SL-CycleGAN generators is demonstrated in Fig. 2. Given a pair of blurry and sharp images  $\{x_i\}_{i=1}^N \in X_{blurry}$  and  $\{y_i\}_{j=1}^M \in Y_{sharp}$ , the generators of SL-CycleGAN learn the translations from  $X_{blurry}$  to  $Y_{sharp}$ . Taking the inspiration from the original CycleGAN model [83], SL-CycleGAN also introduces two generator

networks  $G_X$  and  $G_Y$ . Whereas,  $G_X$  learns the translation function from  $X \rightarrow Y$  such that  $G_X : X_{blur} \rightarrow Y_{sharp}$ . Similarly, the second generator  $G_Y$  learns the mapping from  $Y \rightarrow X$  such that  $G_Y : Y_{sharp} \rightarrow X_{blur}$ . A pair of adversarial discriminators  $D_X$  and  $D_Y$  are also proposed. While  $D_X$  learns to differentiate between the blurry input  $x_i$  and the translated image  $G_Y(\hat{y})$ . Similarly,  $D_Y$  differentiates between the latent sharp image  $y_i$  and the translated image  $G_X(\hat{x})$ . The architecture of our discriminator networks is similar to the PatchGAN  $70 \times 70$  discriminator [24].

### 3.1. Cycle-consistent Deblurring

As mentioned earlier in Sec. 1, GANs have been known for mode collapse. The main reason behind mode collapse in GANs, is its adversarial nature and the choice of the objective function for optimization purposes. Theoretically speaking, a generator function that maps  $G_X : X_{blur} \rightarrow Y_{sharp}$  outputs a distribution of translated image  $p_{data}(\hat{y})$  such that the output image  $\hat{y}$  is similar to the original sharp image  $y$ . The assumption that the generated probability distribution  $p_{data}(\hat{y})$  strictly correlates to the original data distribution  $p_{data}(y)$  requires the generator  $G_X$  to be stochastic in nature [18]. However during inference, such theoretical assumption does not assure that the generator will learn meaningful translations without being the victim of mode collapse.

In order to avoid mode collapse in generators and to improve the optimization ability of the network, Zhu *et al.* [83] argued that the adversarial objective function of generators should be coupled with the term ‘‘cycle-consistent’’. The cycle-consistency term ensures that the generators  $G_X$  and  $G_Y$  are the inverse mapping functions of each other. It can be defined as,

$$L_{cycle}(G_X, G_Y) = \mathbb{E}_{x \sim p_{data}(x)} [\|G_Y(G_X(\hat{x})) - x\|_1] + \mathbb{E}_{y \sim p_{data}(y)} [\|G_X(G_Y(\hat{y})) - y\|_1] \quad (2)$$

where  $L_{cycle}$  in Eq. (2) represents the L1 norm,  $p_{data}(x)$  and  $p_{data}(y)$  represent the distributions of blurry and sharp images.

Unlike our close GAN-based competitors for blind motion deblurring [35, 36, 61, 80], we consider cycle-consistency an essential factor for blind motion deblurring, and show that our network outperforms all the state-of-the-art methods in blind motion dynamic scene deblurring in Sec. 4.

### 3.2. Sparse Convolutions and HTM

The history behind sparse representations is nothing new, in fact, Olshausen *et al.* [49] showed that deploying sparse embeddings and sparse objective functions in encoders can

lead to the representations that are similar to the learnt representations in primate visual cortex. Similarly, Chen *et al.* [10] developed hierarchical sparse representations that are similar to hierarchical feature detectors. The weights for each unit in sparse convolution layers in our Resnet architecture are randomly sampled from a sparse subset of the previous layer. Additionally, the output of each layer is bounded to only  $k$  most non-zero active units. The number of non-zero products in each layer is (sparsity of layer  $l$ ) $\times$ (sparse weights of layer  $l + 1$ ). Fig. 2a represents a conventional arrangement of a residual-block, where each conv layer is followed by InstanceNorm and ReLU as an activation function. Fig. 2b is our modified structure for residual-block, which we called Sparse ResNet-block. To select the most active  $k$  non-zero units and for each unit to be equally active in order to be robust to noise and interference, boosting techniques are applied to sparse convolution layers which can be defined as,

$$c_i^l(t) = (1 - \alpha)c_i^l(t - 1) + \alpha \cdot [i \in topIndices^l] \quad (3)$$

Eq. (3) represents the HTM boosting duty cycle through k-winner, which calculates the running average of each active unit cycle. Where  $c_i^l(t)$  is the unit duty cycles for each unit  $i$  in layer  $l$  at time  $t$ . The boosting coefficient  $b_i^l = e^{\beta(\hat{a}^l - c_i^l(t))}$  is then measured for each unit based on the target and current average duty cycle. Where  $\hat{a}^l$  denotes the number of units that are expected to be active, while the boosting factor  $\beta$  is a positive parameter responsible for controlling the strength of boosting.

In order to construct sparse convolutions with HTM k-winner in Resnet architecture, k-winner is applied to the output of InstanceNorm in each residual-block respectively with stride of 1 and kernel size of  $3 \times 3$ .

### 3.3. Loss functions

In this section, we discuss the loss functions for our proposed SL-CycleGAN, the overall loss function is the combination of three different loss functions.

**Adversarial loss:** The adversarial objective functions is an essential component for blind motion deblurring in GANs. The classic Jensen-Shannon divergence (JSD) based minimax loss function for GANs is proposed by [18] is defined as in Eq. (1). However, the objective function in Eq. (1) suffers from the serious issues such as mode collapse and vanishing gradient. Thus, a conventional minimax objective function is not a good choice for our blind motion deblurring task. Instead, we choose the objective function of [19] with gradient penalty term. The adversarial functions of our proposed network can be defined as follow,

$$L_{adv}(G_X, D_Y, X_{blur}, Y_{sharp}) = \mathbb{E}_{y \sim p_{data}(y)} [D_Y(y)] - \mathbb{E}_{x \sim p_{data}(x)} [D_Y(G_X(x))], \quad (4)$$

$$L_{adv}(G_Y, D_X, Y_{sharp}, X_{blur}) = \mathbb{E}_{x \sim p_{data}(x)} [D_X(x)] - \mathbb{E}_{y \sim p_{data}(y)} [D_X(G_Y(y))] \quad (5)$$

where  $G_X$  and  $G_Y$  are the inverse mapping functions of each other. The adversarial functions for both the generators and discriminators in Eq. (4) and Eq. (5) are combined along with cycle-consistency loss  $L_{cycle}$  from Eq. (3) during the inference.

**Perceptual loss:** We observe that by incorporating only adversarial and cycle-consistency loss, the quality of the restored images is slightly degraded. To further improve the quality of restored images, we adopt the perceptual loss of pre-trained VGG-19 by Johnson *et al.* [27]. The perceptual loss can be defined as,

$$L_{perc} = \frac{1}{W_{i,j} H_{i,j}} \sum_{w=1}^{W_{i,j}} \sum_{h=1}^{H_{i,j}} \left( \phi_{i,j}(I_S)_{w,h} - \phi_{i,j}(G_\theta(I_B))_{w,h} \right)^2 \quad (6)$$

where  $H_{i,j}$  and  $W_{i,j}$  in Eq. (6) indicate the height and width of the conv3×3 layers in the pre-trained VGG19 network.  $\phi_{i,j}$  indicates the obtained feature maps by the j-th convolution layer after the activation function and before the i-th maxpooling layer.  $I_S$  and  $G_\theta(I_B)$  represent the real sharp and the restored deblurred images.

**Overall Loss Function:** The overall loss function for proposed SL-CycleGAN can be defined as,

$$L_{SL-CycleGAN} = L_{adv} + \lambda_{cyc} L_{cycle} + \lambda_{perc} L_{perc} \quad (7)$$

where  $\lambda_{cyc}$  represents the relative coefficient of adversarial functions for  $G_X$  and  $G_Y$ .  $\lambda_{perc}$  is the hyper-parameter for perceptual loss  $L_{perc}$ .

## 4. Experimental evaluation

### 4.1. Experiment settings

We have used Pytorch [53] for all our experiments on Nvidia GTX 1080ti with 11G GPU. We performed experiments on three image benchmarks, GoPro dataset [45], Kohler dataset [32], and Lai dataset [38]. We resized all the images in all three image benchmarks to 256×256 for training and testing and apply data augmentation. For optimization of the generators and the discriminators, we use the Adam optimizer [31] with  $\beta = 0.999$  and batch size of 1. We train our model on all these three image benchmarks for 200 training epochs each with an initial learning rate of 0.0002 for first 100 epochs and linearly decay to zero over next 100 iterations. For all the experiments we set the values of  $\lambda_{cyc} = 10$  and  $\lambda_{perc} = 100$  in Eq. (7). We use the gradient penalty term of [19] for the discriminator networks, which is set to 10. We do not use dropout layer in our modified Sparse ResNet architecture, since [1] in their research show that the utilization of k-winner with sparse

Method	Year	PSNR	SSIM
DeepDeblur [45]	2016	30.12	0.9021
DeblurGAN [35]	2018	28.70	0.958
DeblurGAN-v2-Inception [36]	2019	29.55	0.934
DeblurGAN+ [61]	2020	28.62	0.959
DBGAN [79]	2020	31.10	0.9424
RNNDeblur [78]	2018	29.1872	0.9306
SRN-Deblur [66]	2018	30.26	0.9342
DBCPeNet [7]	2020	31.10	0.945
MTRNN [52]	2019	31.15	0.945
DMPHN [76]	2019	31.50	0.9483
SRN+PSS+NSC [16]	2019	31.58	0.9478
Learning Even-Based Motion Deblurring [25]	2020	31.79	0.949
SAPHNet [62]	2020	32.02	0.953
RADNet [55]	2020	32.15	0.953
BANet [67]	2021	32.44	0.957
MPRNet [75]	2021	32.66	0.959
MIMO-UNet++ [13]	2021	32.68	0.959
HINet [9]	2021	32.71	0.959
SL-CycleGAN (Ours)	2021	<b>38.087</b>	0.954

Table 1. Quantitative comparison of Blind image deblurring on GoPro dataset [45]. Our proposed method SL-CycleGAN achieves the highest PSNR of 38.087 dB on blind image motion deblurring task.

convolutions replaces the need of dropout layers in the network architecture. The training time of our proposed network (SL-CycleGAN) on one dataset for total of 200 training epochs took 2 days to complete, which is 6 days in total for three datasets.

### 4.2. Image Benchmarks

**Evaluation on GoPro Dataset:** GoPro dataset was proposed by Nah *et al.* [45], which consists of 3214 images in total for deblurring task, 2103 training image pairs of blurred and sharp images while the rest of 1111 images are reserved for testing purposes. It is the most commonly used benchmark for blind image deblurring task. The quantitative evaluation on GoPro dataset is presented in Tab. 1. While Tab. 1 presents the timeline of all the state-of-the-art deep learning-based deblurring methods starting from year 2016-2021 both in terms of PSNR and SSIM. Our proposed method SL-CycleGAN outperforms all the state-of-the-art methods on GoPro deblurring task, while achieving



Figure 3. Deblurring results of test images from GoPro dataset. (a) Blurry inputs. (b) Magnified blurry image patches. (c) Corresponding sharp image patches. (d) Deblurring results of [66]. (e) Deblurring results of [35]. (f) Deblurring results of [36]. (g) Deblurring results of [61]. (h) Deblurring results of [80]. (i) Finally, deblurring results of our proposed SL-CycleGAN.

Method	PSNR	SSIM
Whyte <i>et al.</i> [70]	27.02	0.809
Xu <i>et al.</i> [73]	27.40	0.810
Sun <i>et al.</i> [63]	25.21	0.772
DeepDeblur [45]	26.48	0.807
DeblurGAN [35]	25.86	0.802
DeblurGAN-v2 [36]	26.10	0.816
SRN-Deblur [66]	26.75	0.837
DMPHN [76]	24.21	0.7562
Zhang <i>et al.</i> [78]	25.71	0.800
Kim <i>et al.</i> [23]	24.68	0.794
DBCPeNet [7]	26.79	0.839
<b>SL-CycleGAN (ours)</b>	<b>30.818</b>	<b>0.843</b>

Table 2. Quantitative comparison on Kohler dataset [32]. Our proposed SL-CycleGAN achieves significant improvement both in terms of PSNR and SSIM.

the record-breaking PSNR of **38.087** dB, which is 5.377 dB better than the most recent deblurring method HiNet [9]. Similarly, the average SSIM value of our proposed network remains in the list of top five most recent deblurring methods. The qualitative results on GoPro dataset are given in Fig. 3. In comparison with the state-of-the-art blind deblurring methods [35, 36, 61, 66, 80], our proposed approach restores the sharp images from the blurry inputs that are similar to the real sharp images and can be clearly seen in Fig. 3. The resemblance between our restored and the real sharp

Method	PSNR	SSIM
Fergus <i>et al.</i> [15]	22.870	0.682
Cho [11]	23.272	0.699
Xu <i>et al.</i> [73]	25.586	0.773
Krishnan <i>et al.</i> [34]	23.070	0.716
Levin <i>et al.</i> [39]	21.855	0.651
Whyte <i>et al.</i> [70]	23.232	0.667
Sun <i>et al.</i> [63]	24.649	0.756
Xu [72]	25.319	0.765
Zhang <i>et al.</i> [77]	22.918	0.679
Chakrabarti <i>et al.</i> [8]	25.389	0.769
Nah <i>et al.</i> [45]	24.224	0.713
Gong <i>et al.</i> [17]	23.805	0.694
DeblurGAN [35]	24.561	0.741
DeblurGAN-v2 [36]	25.634	0.754
SRN-Deblur [66]	25.231	0.752
<b>SL-CycleGAN (ours)</b>	<b>27.935</b>	<b>0.766</b>

Table 3. Quantitative comparison on Lai dataset [38]. Our Proposed approach shows superior performance than all the other methods in terms of PSNR.

image patches is quite high in comparison with other approaches.

**Evaluation on Kohler Dataset:** Kohler *et al.* [32] proposed a real-world deblurring dataset that consists of 4 latent sharp images and 48 corresponding blurry images of

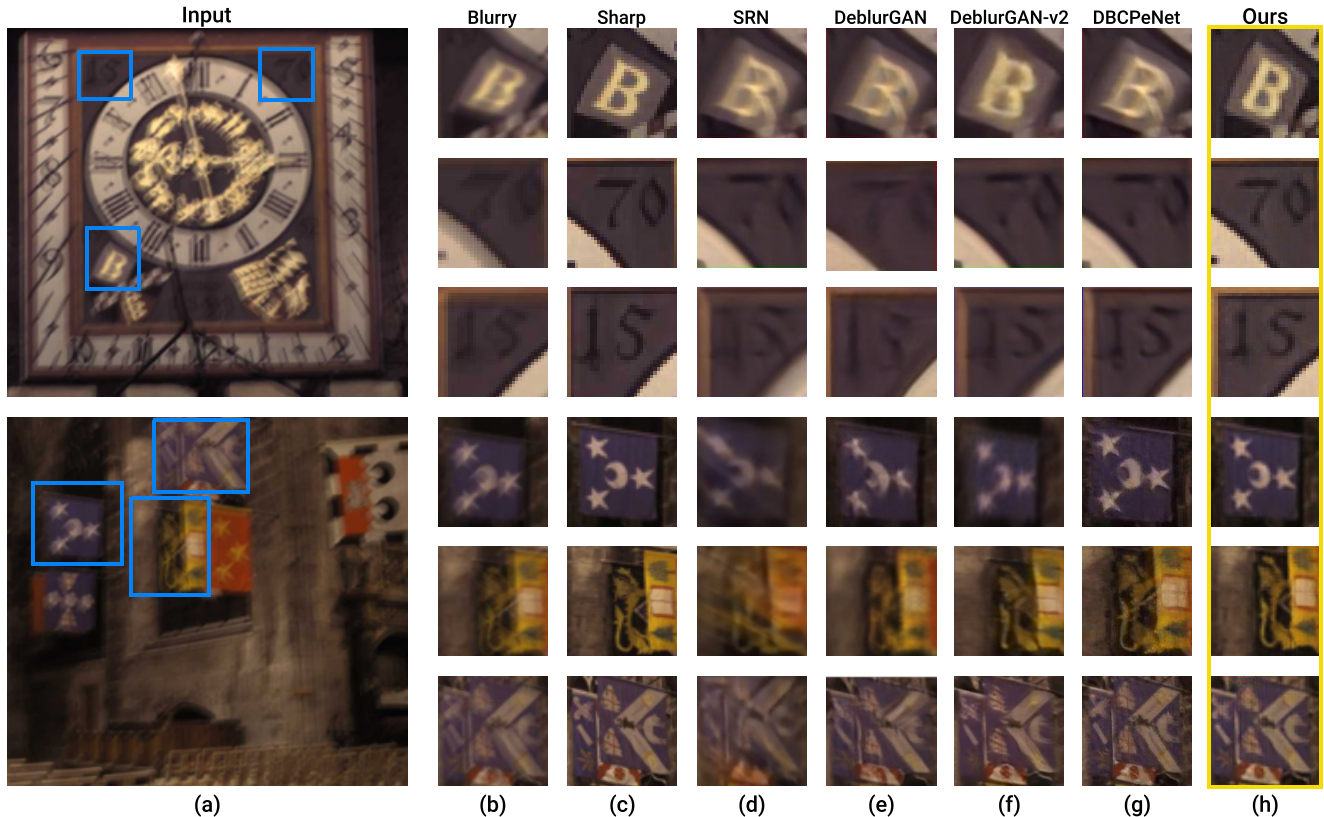


Figure 4. Visual comparison of test images from Kohler dataset [32]. (a) Input blurry images. (b) Magnified blurry image patches. (c) Magnified real sharp image patches. (d) Deblurring results of [66]. (e) Deblurring results of [35]. (f) Deblurring results of [36]. (g) Deblurring results of [7]. (h) Deblurring results of our proposed method.

varying blur kernel intensities. It is the most commonly used benchmark for blind image deblurring comparison. The quantitative comparison of blind image deblurring on Kohler dataset is given in Tab. 2. Our SL-CycleGAN outperforms the other state-of-the-art methods by achieving the average PSNR of 30.818 dB and SSIM of 0.843, while our closest competitor DBCPeNet [7] achieves the PSNR of 26.79 dB and SSIM of 0.839. Similarly, DeblurGAN [35], DeblurGAN-v2 [36], SRN-Deblur [66] and DMPHN [76] show quantitatively inferior performance than our proposed approach. The visual comparison of test images from kohler dataset is presented in Fig. 4. We can see from Fig. 4 that our deblurred sharp image patches retain the texture details and the sharpness similar to the original latent sharp image patches. In comparison with [7, 35, 36, 66], our proposed model shows the ability to understand the distribution of non-uniform blur over different image regions even when the subject of focus lacks significant light reflection.

**Quantitative evaluation on Lai Dataset:** Lai *et al.* [38] proposed a benchmark for blind image deblurring task, which contains 100 real-world blurred images, they also generated synthetic dataset with 200 generated blurred im-

ages containing images of both uniform and non-uniform blur. We present the quantitative comparison on Lai dataset in Tab. 3. We can observe from Tab. 3 that our proposed method achieves 2.301 dB improvement in PSNR than the second highest DeblurGAN-v2 [36]. Meanwhile, the visual results based on the ablation study and analysis on Lai dataset are shown in Fig. 5, which we further discuss in Sec. 4.3 along with the ablation analysis on GoPro and Kohler datasets.

### 4.3. Ablation Study

We conduct an ablation study on the components of SL-CycleGAN and observe the impact and effectiveness of these components both qualitatively and quantitatively. We present the visual ablation study and on three image benchmarks in Fig. 5, while considering original CycleGAN [83] as an starting point. Meanwhile, we gradually keep adding modifications to the generator networks such as replacing standard conv layers in the ResNet by sparse-convs and adding VGG-19 perceptual loss, then eliminating perceptual loss and leaving only sparse conv layers. Finally, we modify the network by integrating perceptual loss, sparse-

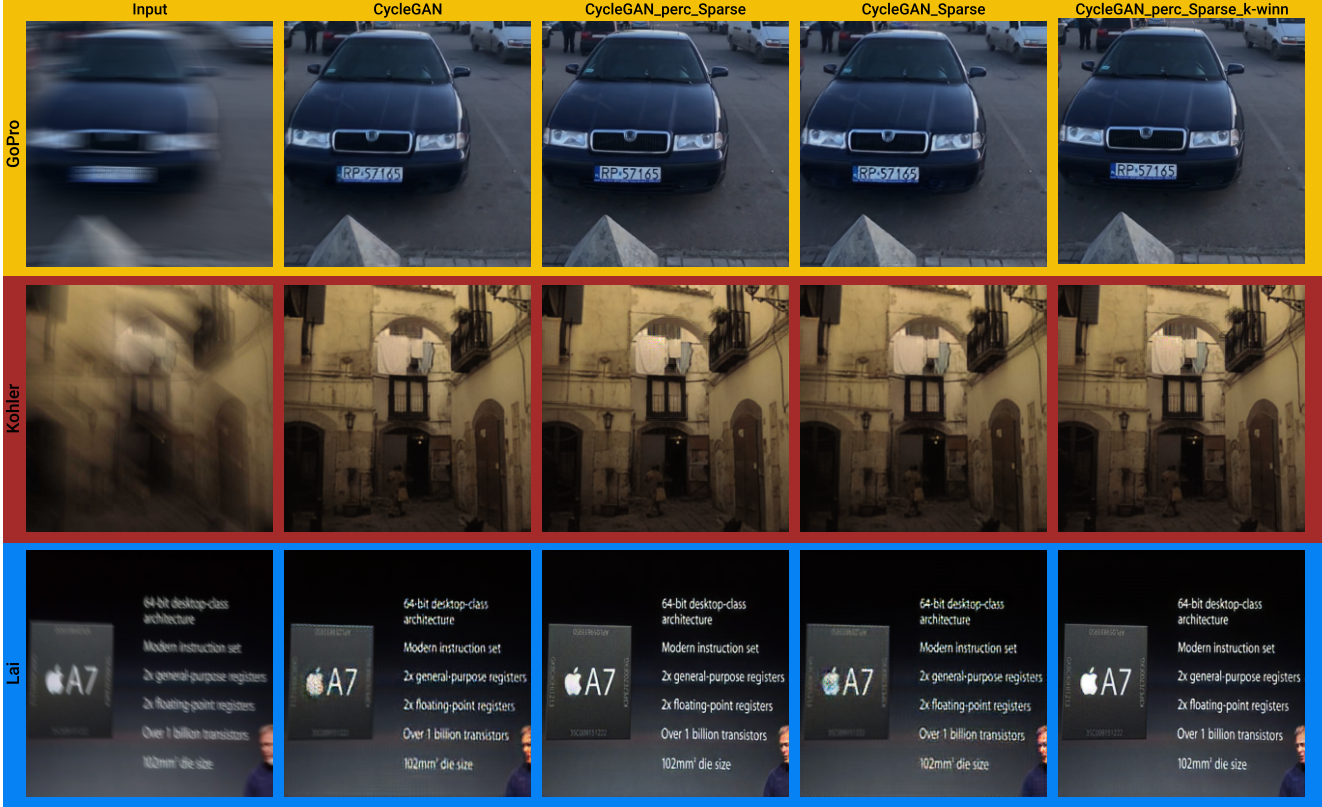


Figure 5. Visual ablation study and analysis on GoPro [45], Kohler [32], and Lai [38] datasets. First row: Images from GoPro. Second row: Images from Kohler dataset. Third row: Images from Lai dataset. Meanwhile the first column represents the blurry inputs, second column: represent deblur results of CycleGAN, third column: CycleGAN with perceptual loss and sparse convs, fourth column: CycleGAN and sparse convs, and finally CycleGAN + perceptual loss + sparse + k-winn (SL-CycleGAN).

GoPro	PSNR(dB)	SSIM	MS-SSIM
CycleGAN	31.835	0.844	0.986
CycleGAN+VGG-19(perceptual)+Sparse	37.852	0.954	0.997
CycleGAN+Sparse	33.135	0.876	0.990
CycleGAN+VGG-19(perceptual)+Sparse+k-winn (SL-CycleGAN)	<b>38.087</b>	0.954	0.997
Kohler			
CycleGAN	29.870	0.814	0.983
CycleGAN+VGG-19(perceptual)+Sparse	29.985	0.814	0.984
CycleGAN+Sparse	30.461	0.823	0.985
CycleGAN+VGG-19(perceptual)+Sparse+k-winn (SL-CycleGAN)	<b>30.818</b>	<b>0.843</b>	<b>0.987</b>
Lai			
CycleGAN	25.034	0.662	0.970
CycleGAN+VGG-19(perceptual)+Sparse	27.581	0.764	0.983
CycleGAN+Sparse	27.564	0.757	0.983
CycleGAN+VGG-19(perceptual)+Sparse+k-winn (SL-CycleGAN)	<b>27.935</b>	<b>0.766</b>	<b>0.984</b>

Table 4. Quantitative ablation study on GoPro [45], Kohler [32] and Lai [38] datasets.

convs and replace ReLU with k-winner in the ResNet generators architecture. We call the final version of our network SL-CycleGAN (CycleGAN + perceptual + sparse-convs +

k-winn). We can see from Fig. 5 that all our sparse versions of the network perform better visually than just CycleGAN, especially the final version SL-CycleGAN produces visually appealing results. Similarly in Tab. 4 of ablation study, SL-CycleGAN outperforms all the preceding versions quantitatively.

**Limitations:** Keeping in mind that “Honesty is the best policy”. We observe that during the inference on GoPro dataset, some of the restored images by SL-CycleGAN show slightly dim light in comparison with the original bright sharp images. However, we consider it as an inherited issue from the original CycleGAN and cycle-consistency loss [83].

## 5. Conclusion

This paper introduces a novel blind image deblurring network SL-CycleGAN, that for the first time, utilizes sparse representation learning with HTM k-winner for improved image deblurring and is more robust towards noise and interference. Meanwhile, achieving the best qualitative and quantitative results on popular image benchmarks.

## References

- [1] Subutai Ahmad and Luiz Scheinkman. How can we be so dense? the benefits of using highly sparse representations. *arXiv preprint arXiv:1903.11257*, 2019. 2, 5
- [2] Raied Aljadaany, Dipan K Pal, and Marios Savvides. Douglas-rachford networks: Learning both the image prior and data fidelity terms for blind image deconvolution. In *Proceedings of the IEEE/CVF Conference on Computer Vision and Pattern Recognition*, pages 10235–10244, 2019. 3
- [3] Martin Arjovsky and Léon Bottou. Towards principled methods for training generative adversarial networks. *arXiv preprint arXiv:1701.04862*, 2017. 2
- [4] Martin Arjovsky, Soumith Chintala, and Léon Bottou. Wasserstein generative adversarial networks. In *International conference on machine learning*, pages 214–223. PMLR, 2017. 3
- [5] Muhammad Asim, Fahad Shamshad, and Ali Ahmed. Blind image deconvolution using deep generative priors. *IEEE Transactions on Computational Imaging*, 6:1493–1506, 2020. 2, 3
- [6] John Bardsley, Stuart Jefferies, James Nagy, and Robert Plemmons. Blind iterative restoration of images with spatially-varying blur. *Optics Express*, 14(5):1767–1782, 2006. 1
- [7] Jianrui Cai, Wangmeng Zuo, and Lei Zhang. Dark and bright channel prior embedded network for dynamic scene deblurring. *IEEE Transactions on Image Processing*, 29:6885–6897, 2020. 2, 5, 6, 7
- [8] Ayan Chakrabarti, Todd Zickler, and William T Freeman. Analyzing spatially-varying blur. In *2010 IEEE Computer Society Conference on Computer Vision and Pattern Recognition*, pages 2512–2519. IEEE, 2010. 6
- [9] Liangyu Chen, Xin Lu, Jie Zhang, Xiaojie Chu, and Chengpeng Chen. Hinet: Half instance normalization network for image restoration. In *Proceedings of the IEEE/CVF Conference on Computer Vision and Pattern Recognition*, pages 182–192, 2021. 5, 6
- [10] Yubei Chen, Dylan M Paiton, and Bruno A Olshausen. The sparse manifold transform. *arXiv preprint arXiv:1806.08887*, 2018. 4
- [11] Sunghyun Cho and Seungyong Lee. Fast motion deblurring. In *ACM SIGGRAPH Asia 2009 papers*, pages 1–8. 2009. 2, 6
- [12] Sunghyun Cho, Yasuyuki Matsushita, and Seungyong Lee. Removing non-uniform motion blur from images. In *2007 IEEE 11th International Conference on Computer Vision*, pages 1–8. IEEE, 2007. 1
- [13] Sung-Jin Cho, Seo-Won Ji, Jun-Pyo Hong, Seung-Won Jung, and Sung-Jea Ko. Rethinking coarse-to-fine approach in single image deblurring. In *Proceedings of the IEEE/CVF International Conference on Computer Vision*, pages 4641–4650, 2021. 5
- [14] Florent Couzinié-Devy, Jian Sun, Karteek Alahari, and Jean Ponce. Learning to estimate and remove non-uniform image blur. In *Proceedings of the IEEE Conference on Computer Vision and Pattern Recognition*, pages 1075–1082, 2013. 1
- [15] Rob Fergus, Barun Singh, Aaron Hertzmann, Sam T Roweis, and William T Freeman. Removing camera shake from a single photograph. *ACM Transactions on Graphics (TOG)*, 25(3):787–794, 2006. 2, 6
- [16] Hongyun Gao, Xin Tao, Xiaoyong Shen, and Jiaya Jia. Dynamic scene deblurring with parameter selective sharing and nested skip connections. In *Proceedings of the IEEE/CVF Conference on Computer Vision and Pattern Recognition*, pages 3848–3856, 2019. 2, 5
- [17] Dong Gong, Jie Yang, Lingqiao Liu, Yanning Zhang, Ian Reid, Chunhua Shen, Anton Van Den Hengel, and Qinfeng Shi. From motion blur to motion flow: A deep learning solution for removing heterogeneous motion blur. In *Proceedings of the IEEE conference on computer vision and pattern recognition*, pages 2319–2328, 2017. 2, 6
- [18] Ian Goodfellow, Jean Pouget-Abadie, Mehdi Mirza, Bing Xu, David Warde-Farley, Sherjil Ozair, Aaron Courville, and Yoshua Bengio. Generative adversarial nets. In *Advances in Neural Information Processing Systems*, volume 27, pages 2672–2680, 2014. 1, 2, 4
- [19] Ishaan Gulrajani, Faruk Ahmed, Martin Arjovsky, Vincent Dumoulin, and Aaron Courville. Improved training of wasserstein gans. In *Proceedings of the 31st International Conference on Neural Information Processing Systems*, pages 5769–5779, 2017. 3, 4, 5
- [20] Jeff Hawkins. A thousand brains: A new theory of intelligence, 2021. 2
- [21] Jeff Hawkins, Subutai Ahmad, Donna Dubinsky, et al. Cortical learning algorithm and hierarchical temporal memory. *Numenta Whitepaper*, 1:68, 2011. 2
- [22] Michael Hirsch, Christian J Schuler, Stefan Harmeling, and Bernhard Schölkopf. Fast removal of non-uniform camera shake. In *2011 International Conference on Computer Vision*, pages 463–470. IEEE, 2011. 1
- [23] Tae Hyun Kim, Byeongjoo Ahn, and Kyoung Mu Lee. Dynamic scene deblurring. In *Proceedings of the IEEE International Conference on Computer Vision*, pages 3160–3167, 2013. 6
- [24] Phillip Isola, Jun-Yan Zhu, Tinghui Zhou, and Alexei A Efros. Image-to-image translation with conditional adversarial networks. In *Proceedings of the IEEE conference on computer vision and pattern recognition*, pages 1125–1134, 2017. 4
- [25] Zhe Jiang, Yu Zhang, Dongqing Zou, Jimmy Ren, Jiancheng Lv, and Yebin Liu. Learning event-based motion deblurring. In *Proceedings of the IEEE/CVF Conference on Computer Vision and Pattern Recognition*, pages 3320–3329, 2020. 5
- [26] Jianbo Jiao, Wei-Chih Tu, Shengfeng He, and Rynson WH Lau. Formresnet: Formatted residual learning for image restoration. In *Proceedings of the IEEE Conference on Computer Vision and Pattern Recognition Workshops*, pages 38–46, 2017. 3
- [27] Justin Johnson, Alexandre Alahi, and Li Fei-Fei. Perceptual losses for real-time style transfer and super-resolution. In *European conference on computer vision*, pages 694–711. Springer, 2016. 5

- [28] Alexia Jolicœur-Martineau. The relativistic discriminator: a key element missing from standard gan. In *International Conference on Learning Representations*, 2018. 3
- [29] Tero Karras, Samuli Laine, and Timo Aila. A style-based generator architecture for generative adversarial networks. In *Proceedings of the IEEE/CVF Conference on Computer Vision and Pattern Recognition*, pages 4401–4410, 2019. 1
- [30] Tero Karras, Samuli Laine, Miika Aittala, Janne Hellsten, Jaakko Lehtinen, and Timo Aila. Analyzing and improving the image quality of stylegan. In *Proceedings of the IEEE/CVF Conference on Computer Vision and Pattern Recognition*, pages 8110–8119, 2020. 1
- [31] Diederik P Kingma and Jimmy Ba. Adam: A method for stochastic optimization. *arXiv preprint arXiv:1412.6980*, 2014. 5
- [32] Rolf Köhler, Michael Hirsch, Betty Mohler, Bernhard Schölkopf, and Stefan Harmeling. Recording and playback of camera shake: Benchmarking blind deconvolution with a real-world database. In *European conference on computer vision*, pages 27–40. Springer, 2012. 5, 6, 7, 8
- [33] Dilip Krishnan and Rob Fergus. Fast image deconvolution using hyper-laplacian priors, supplementary material. In *Neural Information Pro-cessing Systems Conference*. Cite-seer, 2009. 1
- [34] Dilip Krishnan, Terence Tay, and Rob Fergus. Blind deconvolution using a normalized sparsity measure. In *CVPR 2011*, pages 233–240. IEEE, 2011. 2, 6
- [35] Orest Kupyn, Volodymyr Budzan, Mykola Mykhailych, Dmytro Mishkin, and Jiří Matas. Deblurgan: Blind motion deblurring using conditional adversarial networks. In *Proceedings of the IEEE conference on computer vision and pattern recognition*, pages 8183–8192, 2018. 2, 3, 4, 5, 6, 7
- [36] Orest Kupyn, Tetiana Martyniuk, Junru Wu, and Zhangyang Wang. Deblurgan-v2: Deblurring (orders-of-magnitude) faster and better. In *Proceedings of the IEEE/CVF International Conference on Computer Vision*, pages 8878–8887, 2019. 1, 2, 3, 4, 5, 6, 7
- [37] Reginald L Lagendijk and Jan Biemond. Basic methods for image restoration and identification. In *The essential guide to image processing*, pages 323–348. Elsevier, 2009. 1
- [38] Wei-Sheng Lai, Jia-Bin Huang, Zhe Hu, Narendra Ahuja, and Ming-Hsuan Yang. A comparative study for single image blind deblurring. In *Proceedings of the IEEE Conference on Computer Vision and Pattern Recognition*, pages 1701–1709, 2016. 5, 6, 7, 8
- [39] Anat Levin, Yair Weiss, Fredo Durand, and William T Freeman. Understanding and evaluating blind deconvolution algorithms. In *2009 IEEE Conference on Computer Vision and Pattern Recognition*, pages 1964–1971. IEEE, 2009. 6
- [40] Anat Levin, Yair Weiss, Fredo Durand, and William T Freeman. Efficient marginal likelihood optimization in blind deconvolution. In *CVPR 2011*, pages 2657–2664. IEEE, 2011. 1, 2
- [41] Lerenhan Li, Jinshan Pan, Wei-Sheng Lai, Changxin Gao, Nong Sang, and Ming-Hsuan Yang. Learning a discriminative prior for blind image deblurring. In *Proceedings of the IEEE Conference on Computer Vision and Pattern Recognition*, pages 6616–6625, 2018. 3
- [42] Jen-Chun Lin, Wen-Li Wei, Tyng-Luh Liu, C-C Jay Kuo, and Mark Liao. Tell me where it is still blurry: Adversarial blurred region mining and refining. In *Proceedings of the 27th ACM International Conference on Multimedia*, pages 702–710, 2019. 3
- [43] Tsung-Yi Lin, Piotr Dollár, Ross Girshick, Kaiming He, Bharath Hariharan, and Serge Belongie. Feature pyramid networks for object detection. In *Proceedings of the IEEE conference on computer vision and pattern recognition*, pages 2117–2125, 2017. 3
- [44] Tomer Michaeli and Michal Irani. Blind deblurring using internal patch recurrence. In *European conference on computer vision*, pages 783–798. Springer, 2014. 2
- [45] Seungjun Nah, Tae Hyun Kim, and Kyoung Mu Lee. Deep multi-scale convolutional neural network for dynamic scene deblurring. In *Proceedings of the IEEE conference on computer vision and pattern recognition*, pages 3883–3891, 2017. 1, 2, 5, 6, 8
- [46] NASA. <https://photojournal.jpl.nasa.gov/>. 1
- [47] Shree K Nayar and Moshe Ben-Ezra. Motion-based motion deblurring. *IEEE transactions on pattern analysis and machine intelligence*, 26(6):689–698, 2004. 1
- [48] Mehdi Noroozi, Paramanand Chandramouli, and Paolo Favaro. Motion deblurring in the wild. In *German conference on pattern recognition*, pages 65–77. Springer, 2017. 2
- [49] Bruno A Olshausen and David J Field. Sparse coding with an overcomplete basis set: A strategy employed by v1? *Vision research*, 37(23):3311–3325, 1997. 4
- [50] Jinshan Pan, Zhe Hu, Zhixun Su, and Ming-Hsuan Yang.  $l_0$ -regularized intensity and gradient prior for deblurring text images and beyond. *IEEE transactions on pattern analysis and machine intelligence*, 39(2):342–355, 2016. 2
- [51] Jinshan Pan, Deqing Sun, Hanspeter Pfister, and Ming-Hsuan Yang. Blind image deblurring using dark channel prior. In *Proceedings of the IEEE Conference on Computer Vision and Pattern Recognition*, pages 1628–1636, 2016. 1, 2
- [52] Dongwon Park, Dong Un Kang, Jisoo Kim, and Se Young Chun. Multi-temporal recurrent neural networks for progressive non-uniform single image deblurring with incremental temporal training. In *European Conference on Computer Vision*, pages 327–343. Springer, 2020. 5
- [53] Adam Paszke, Sam Gross, Francisco Massa, Adam Lerer, James Bradbury, Gregory Chanan, Trevor Killeen, Zeming Lin, Natalia Gimelshein, Luca Antiga, Alban Desmaison, Andreas Kopf, Edward Yang, Zachary DeVito, Martin Raison, Alykhan Tejani, Sasank Chilamkurthy, Benoit Steiner, Lu Fang, Junjie Bai, and Soumith Chintala. Pytorch: An imperative style, high-performance deep learning library. In H. Wallach, H. Larochelle, A. Beygelzimer, F. d’Alché-Buc, E. Fox, and R. Garnett, editors, *Advances in Neural Information Processing Systems 32*, pages 8024–8035. Curran Associates, Inc., 2019. 5
- [54] Daniele Perrone and Paolo Favaro. A logarithmic image prior for blind deconvolution. *International journal of computer vision*, 117(2):159–172, 2016. 2

- [55] Kuldeep Purohit and AN Rajagopalan. Region-adaptive dense network for efficient motion deblurring. In *Proceedings of the AAAI Conference on Artificial Intelligence*, volume 34, pages 11882–11889, 2020. 5
- [56] Alec Radford, Luke Metz, and Soumith Chintala. Un-supervised representation learning with deep convolutional generative adversarial networks. *arXiv preprint arXiv:1511.06434*, 2015. 2
- [57] Dongwei Ren, Kai Zhang, Qilong Wang, Qinghua Hu, and Wangmeng Zuo. Neural blind deconvolution using deep priors. In *Proceedings of the IEEE/CVF Conference on Computer Vision and Pattern Recognition*, pages 3341–3350, 2020. 3
- [58] William Hadley Richardson. Bayesian-based iterative method of image restoration. *Journal of the Optical Society of America (1917-1983)*, 62(1):55, 1972. 1
- [59] Christian J Schuler, Michael Hirsch, Stefan Harmeling, and Bernhard Schölkopf. Learning to deblur. *IEEE transactions on pattern analysis and machine intelligence*, 38(7):1439–1451, 2015. 1, 2
- [60] Qi Shan, Jiaya Jia, and Aseem Agarwala. High-quality motion deblurring from a single image. *Acm transactions on graphics (tog)*, 27(3):1–10, 2008. 1, 2
- [61] Wen-Ze Shao, Yuan-Yuan Liu, Lu-Yue Ye, Li-Qian Wang, Qi Ge, Bing-Kun Bao, and Hai-Bo Li. Deblurgan+: revisiting blind motion deblurring using conditional adversarial networks. *Signal Processing*, 168:107338, 2020. 2, 3, 4, 5, 6
- [62] Maitreya Suin, Kuldeep Purohit, and AN Rajagopalan. Spatially-attentive patch-hierarchical network for adaptive motion deblurring. In *Proceedings of the IEEE/CVF Conference on Computer Vision and Pattern Recognition*, pages 3606–3615, 2020. 5
- [63] Jian Sun, Wenfei Cao, Zongben Xu, and Jean Ponce. Learning a convolutional neural network for non-uniform motion blur removal. In *Proceedings of the IEEE Conference on Computer Vision and Pattern Recognition*, pages 769–777, 2015. 1, 2, 6
- [64] Libin Sun, Sunghyun Cho, Jue Wang, and James Hays. Edge-based blur kernel estimation using patch priors. In *IEEE International Conference on Computational Photography (ICCP)*, pages 1–8. IEEE, 2013. 2
- [65] Christian Szegedy, Sergey Ioffe, Vincent Vanhoucke, and Alexander Alemi. Inception-v4, inception-resnet and the impact of residual connections on learning. In *Proceedings of the AAAI Conference on Artificial Intelligence*, volume 31, 2017. 3
- [66] Xin Tao, Hongyun Gao, Xiaoyong Shen, Jue Wang, and Jiaya Jia. Scale-recurrent network for deep image deblurring. In *Proceedings of the IEEE Conference on Computer Vision and Pattern Recognition*, pages 8174–8182, 2018. 1, 2, 5, 6, 7
- [67] Fu-Jen Tsai, Yan-Tsung Peng, Yen-Yu Lin, Chung-Chi Tsai, and Chia-Wen Lin. Banet: Blur-aware attention networks for dynamic scene deblurring. *arXiv preprint arXiv:2101.07518*, 2021. 5
- [68] Ruxin Wang and Dacheng Tao. Recent progress in image deblurring. *arXiv preprint arXiv:1409.6838*, 2014. 1
- [69] Manuel Werlberger, Thomas Pock, and Horst Bischof. Motion estimation with non-local total variation regularization. In *2010 IEEE Computer Society Conference on Computer Vision and Pattern Recognition*, pages 2464–2471. IEEE, 2010. 1
- [70] Oliver Whyte, Josef Sivic, Andrew Zisserman, and Jean Ponce. Non-uniform deblurring for shaken images. *International journal of computer vision*, 98(2):168–186, 2012. 6
- [71] Norbert Wiener. *Extrapolation, interpolation, and smoothing of stationary time series: with engineering applications*. MIT press Cambridge, 1950. 1
- [72] Li Xu and Jiaya Jia. Two-phase kernel estimation for robust motion deblurring. In *European conference on computer vision*, pages 157–170. Springer, 2010. 2, 6
- [73] Li Xu, Shicheng Zheng, and Jiaya Jia. Unnatural l0 sparse representation for natural image deblurring. In *Proceedings of the IEEE conference on computer vision and pattern recognition*, pages 1107–1114, 2013. 1, 2, 6
- [74] Yitzhak Yitzhaky and Norman S Kopeika. Identification of blur parameters from motion blurred images. *Graphical models and image processing*, 59(5):310–320, 1997. 1
- [75] Syed Waqas Zamir, Aditya Arora, Salman Khan, Munawar Hayat, Fahad Shahbaz Khan, Ming-Hsuan Yang, and Ling Shao. Multi-stage progressive image restoration. In *Proceedings of the IEEE/CVF Conference on Computer Vision and Pattern Recognition*, pages 14821–14831, 2021. 5
- [76] Hongguang Zhang, Yuchao Dai, Hongdong Li, and Piotr Koniusz. Deep stacked hierarchical multi-patch network for image deblurring. In *Proceedings of the IEEE/CVF Conference on Computer Vision and Pattern Recognition*, pages 5978–5986, 2019. 2, 5, 6, 7
- [77] Haichao Zhang, David Wipf, and Yanning Zhang. Multi-image blind deblurring using a coupled adaptive sparse prior. In *Proceedings of the IEEE Conference on Computer Vision and Pattern Recognition*, pages 1051–1058, 2013. 6
- [78] Jiawei Zhang, Jinshan Pan, Jimmy Ren, Yibing Song, Linchao Bao, Rynson WH Lau, and Ming-Hsuan Yang. Dynamic scene deblurring using spatially variant recurrent neural networks. In *Proceedings of the IEEE Conference on Computer Vision and Pattern Recognition*, pages 2521–2529, 2018. 1, 2, 5, 6
- [79] Kaihao Zhang, Wenhan Luo, Yiran Zhong, Lin Ma, Bjorn Stenger, Wei Liu, and Hongdong Li. Deblurring by realistic blurring. In *Proceedings of the IEEE/CVF Conference on Computer Vision and Pattern Recognition*, pages 2737–2746, 2020. 5
- [80] Shuang Zhang, Ada Zhen, and Robert L Stevenson. Deep motion blur removal using noisy/blurry image pairs. *Journal of Electronic Imaging*, 30(3):033022, 2021. 2, 3, 4, 6
- [81] Xinyi Zhang, Hang Dong, Zhe Hu, Wei Sheng Lai, Fei Wang, and Ming Hsuan Yang. Gated fusion network for joint image deblurring and super-resolution. In *29th British Machine Vision Conference, BMVC 2018*, 2019. 3
- [82] Xinxin Zhang, Ronggang Wang, Yonghong Tian, Wenmin Wang, and Wen Gao. Image deblurring using robust sparsity priors. In *2015 IEEE International Conference on Image Processing (ICIP)*, pages 138–142. IEEE, 2015. 1

- [83] Jun-Yan Zhu, Taesung Park, Phillip Isola, and Alexei A Efros. Unpaired image-to-image translation using cycle-consistent adversarial networks. In *Proceedings of the IEEE international conference on computer vision*, pages 2223–2232, 2017. [2](#), [3](#), [4](#), [7](#), [8](#)
- [84] Daniel Zoran and Yair Weiss. From learning models of natural image patches to whole image restoration. In *2011 International Conference on Computer Vision*, pages 479–486. IEEE, 2011. [1](#)